Title: Tree height and leaf drought tolerance traits shape growth responses across droughts in a temperate broadleaf forest

Authors: Ian R. McGregor[1,2], Ryan Helcoski[1], Norbert Kunert[1,3], Alan J. Tepley[1,4], Erika B. Gonzalez-Akre[1], Valentine Herrmann[1], Joseph Zailaa[1,5], Atticus E.L. Stovall[1,6,7], Norman A. Bourg[1], William J. McShea[1], Neil Pederson[8], Lawren Sack[9,10], Kristina J. Anderson-Teixeira[1,3]*

Author Affiliations:

1. Conservation Ecology Center; Smithsonian Conservation Biology Institute; National Zoological Park, Front Royal, VA 22630, USA
2. Center for Geospatial Analytics; North Carolina State University; Raleigh, NC 27607, USA
3. Center for Tropical Forest Science-Forest Global Earth Observatory; Smithsonian Tropical Research Institute; Panama, Republic of Panama
4. Canadian Forest Service, Northern Forestry Centre, Edmonton, Alberta, Canada T6H 3S5
5. Biological Sciences Department; California State University; Los Angeles, CA 90032, USA
6. Department of Environmental Sciences, University of Virginia, Charlottesville, VA 22903, USA
7. NASA Goddard Space Flight Center; Greenbelt, MD 20771, USA
8. Harvard Forest, Petersham, MA 01366, USA
9. Department of Ecology and Evolutionary Biology; University of California, Los Angeles; Los Angeles, CA 90095, USA
10. Institute of the Environment and Sustainability; University of California, Los Angeles; Los Angeles, CA 90095, USA

*corresponding author: teixeirak@si.edu; +1 540 635 6546

Text	word count	other	n
Total word count (excluding summary, references and legends)	6,494	No. of figures	4 (all colour)
Summary	200	No. of Tables	3
Introduction	1,347	No of Supporting Information files	19
Materials and Methods	2,057		
Results	1129		
Discussion	1955		
Acknowledgments	142		

Summary

- As climate change drives increased drought in many forested regions, mechanistic understanding of the factors conferring drought tolerance in trees is increasingly important. The dendrochronological record provides a window through which we can understand how tree size and traits shape growth responses to droughts.
- We analyzed tree-ring records for twelve species in a broadleaf deciduous forest in Virginia (USA) to test hypotheses for how tree height, microenvironment characteristics, and species' traits shaped drought responses across the three strongest regional droughts over a 60-year period.
- Drought tolerance (resistance, recovery, and resilience) decreased with tree height, which was strongly correlated with exposure to higher solar radiation and evaporative demand. The potentially greater rooting volume of larger trees did not confer a resistance advantage, but marginally increased recovery and resilience, in sites with low topographic wetness index. Drought tolerance was greater among species whose leaves lost turgor (wilted) at more negative water potentials and experienced less shrinkage upon desiccation.
- The tree-ring record reveals that tree height and leaf drought tolerance traits influenced growth responses during and after significant droughts in the meteorological record. As climate change-induced droughts intensify, tall trees with drought-sensitive leaves will be most vulnerable to immediate and longer-term growth reductions.

Key words: annual growth; crown exposure; drought; Forest Global Earth Observatory (ForestGEO); leaf drought tolerance traits; temperate broadleaf deciduous forest; tree height; tree-ring

Introduction

Forests play a critical global role in climate regulation (Bonan, 2008), yet there remains enormous uncertainty as to how the forest-dominated terrestrial carbon sink will respond to climate change (Friedlingstein *et al.*, 2006). An important aspect of this uncertainty lies with physiological responses of trees to drought (Kennedy *et al.*, 2019). In many forested regions around the world, the risk of severe drought is increasing (Trenberth *et al.*, 2014; Dai *et al.*, 2018), often despite increasing precipitation (Intergovernmental Panel on Climate Change, 2015; Cook *et al.*, 2015). Droughts, intensified by climate change, have been affecting forests worldwide and are expected to continue as an important driver of forest change (Allen *et al.*, 2015, 2010; McDowell *et al.*, 2020). Understanding forest responses to drought requires elucidation of how tree size, microenvironment, and species' traits jointly influence individual-level drought tolerance, defined here as a tree's ability to maintain growth during drought (*resistance*), increase growth relative to drought minimum (*recovery*), and re-establish its pre-drought growth rate (*resilience*; Lloret *et al.*, 2011). Survival has been shown to be linked to resistance, recovery, and resilience (DeSoto *et al.*, 2020; Gessler *et al.*, 2020), implying they may be influenced by the same factors. However, it has proven difficult to resolve the many factors affecting tree growth during drought and the extent to which their influence is consistent across droughts. This is because available forest census data only rarely captures extreme drought, whereas tree-ring records capture multiple droughts but typically focus on only the largest individuals of one or a few species.

Many studies have shown that within and across species, large trees tend to be more affected by drought. Greater growth reductions (*i.e.*, lower drought resistance) in larger trees were first shown on a global scale by Bennett *et al.* (2015), and subsequent studies have reinforced this finding (*e.g.*, Pretzsch *et al.*, 2018; Gillerot *et al.*, 2020). Although lower recovery and resilience of larger trees have also been observed (Gillerot *et al.*, 2020), results were mixed (Merlin *et al.*, 2015), and a recent physiological model suggests that large trees destined to die following drought may still exhibit high recovery and resilience (Trugman *et al.*, 2018). Thus, in general we have much more limited understanding of how and why drought resilience scales with tree size.

Moreover, it has yet to be resolved which of several potential underlying mechanisms most strongly shape these trends in drought response. First, tree height itself may be a primary driver. Taller trees face the biophysical challenge of lifting water greater distances against the effects of gravity and friction (Ryan *et al.*, 2006; McDowell *et al.*, 2011; Couvreur *et al.*, 2018; McDowell & Allen, 2015). Vertical gradients in stem and leaf traits–including smaller and thicker leaves (higher leaf mass per area), greater resistance to hydraulic dysfunction (*i.e.*, more negative water potential at 50% loss of hydraulic conductivity, more negative P50), and the tapering of hydraulic conductivity at greater heights (McDowell *et al.*, 2011; Couvreur *et al.*, 2018; Koike *et al.*, 2001)–enable trees to become tall (Couvreur *et al.*, 2018). Greater stem capacitance (*i.e.*, water storage capacity) of larger trees may also confer resistance to transient droughts (Scholz *et al.*, 2011; Phillips *et al.*, 2003). Taller trees have wider conduits in the basal portions of taller trees, both within and across species (Olson *et al.*, 2018; Liu *et al.*, 2019) and throughout the conductive systems of angiosperms (Zach *et al.*, 2010; Olson *et al.*, 2014, 2018), which help maintain constant the resistance that would otherwise increase as trees grow taller. Wider xylem conduits plausibly make large trees more vulnerable to embolism during drought (Olson *et al.*, 2018), and traits conducive to efficient water transport may also lead to poor ability to recover from or re-route water around embolisms (Roskilly *et al.*, 2019).

Larger trees may also have lower drought tolerance because of microenvironmental and ecological factors. Their crowns tend to occupy more exposed canopy positions, which are associated with higher evaporative demand (Kunert *et al.*, 2017). Counteracting the liabilities associated with tall height, large trees tend to

have larger root systems (Enquist & Niklas, 2002; Hui *et al.*, 2014), potentially mitigating some of the biophysical challenges they face by allowing greater access to water. Larger root systems–if they grant access to deeper water sources–would be particularly advantageous in drier microenvironments (e.g., hilltops, as compared to valleys and streambeds) during drought. Finally, tree size-related responses to drought can be modified by species' traits and their distribution across size classes (Meakem *et al.*, 2018; Liu *et al.*, 2019). Understanding the mechanisms driving the greater relative growth reductions of larger trees during drought requires disentangling the interactive effects of height and associated exposure, root water access, and species' traits.

Debates have also arisen regarding the traits influencing tree growth responses to drought. Studies within temperate broadleaf forests have observed ring-porous species showing higher drought tolerance than diffuse-porous species (Kannenberg *et al.*, 2019; Friedrichs *et al.*, 2009; Elliott *et al.*, 2015). However, this differentiation is not universal within the biome (Martin-Benito & Pederson, 2015), does not hold in the global context (Wheeler *et al.*, 2007; Olson *et al.*, 2020), and does not resolve differences among the many species within each category. Commonly-measured traits including wood density (WD) and leaf mass per area (LMA) have been linked to drought responses within some temperate deciduous forests (Hoffmann *et al.*, 2011; Martin-Benito & Pederson, 2015; Abrams, 1990; Guerfel *et al.*, 2009) and across forests worldwide (Greenwood *et al.*, 2017). However, in other cases these traits could not explain drought tolerance (e.g., in a tropical rainforest; Maréchaux *et al.*, 2019), or the direction of response was not always consistent. For instance, higher wood density has been associated with greater drought resistance at a global scale (Greenwood *et al.*, 2017), but correlated negatively with tree performance during drought in a broadleaf deciduous forest in the southeastern United States (Hoffmann *et al.*, 2011). Thus, the perceived influence of these traits on drought resistance may actually reflect indirect correlations with other traits that more directly drive drought responses (Hoffmann *et al.*, 2011).

In contrast, hydraulic traits have direct physiological linkages to tree growth and mortality responses to drought. For instance, water potentials at which the percent loss of conductivity surpasses a certain threshold (e.g., P50 and P88, representing 50 and 88% loss of conductivity, respectively) and hydraulic safety margin (*i.e.*, difference between typical minimum water potentials and P50 or P88) correlate with drought performance across global forests (Anderegg *et al.*, 2016). However, these are time-consuming to measure and therefore often infeasible for predicting or modeling drought responses in highly diverse forests (*e.g.*, in the tropics). More easily-measurable leaf drought tolerance traits that have direct linkage to plant hydraulic function can explain variation in plant distribution and function (Medeiros *et al.*, 2019). These include leaf area shrinkage upon desiccation (PLA_{dry}; Scoffoni *et al.*, 2014) and the leaf water potential at turgor loss point (π_{tlp}), *i.e.,* the water potential at which leaf wilting occurs (Bartlett *et al.*, 2016a; Zhu *et al.*, 2018). Both traits correlate with hydraulic vulnerability and drought tolerance as part of unified plant hydraulic systems (Farrell *et al.*, 2017; Scoffoni *et al.*, 2014; Bartlett *et al.*, 2016a; Zhu *et al.*, 2018). The abilities of both PLA_{dry} and π_{tlp} to explain the drought tolerance of tree growth remains untested (but see Powers *et al.*, 2020 for π_{tlp} link to mortality).

Here, we examine how tree height, microenvironment characteristics, and species' traits collectively shape three metrics of drought tolerance: (1) resistance, defined as the ratio of annual stem growth in a drought year to that which would be expected in the absence of drought from previous growth; (2) recovery, defined as the ratio of post-drought growth to growth during the drought year; and (3) resilience, defined as the ratio of post-drought to pre-drought growth (Lloret *et al.*, 2011). We test a series of hypotheses and associated

specific predictions (Table 1) based on the combination of tree-ring records from the three strongest droughts over a 60-year period (1950 - 2009), species trait measurements, and census and microenvironmental data from a large forest dynamics plot in Virginia, USA. First, we focus on how tree size, alone and in its interaction with microenvironmental gradients, influences drought tolerance. We examine the contemporary relationship between tree height and microenvironment, including growing season meteorological conditions and crown exposure. We then test whether, consistent with most forests globally, larger-diameter, taller trees tend to have lower drought tolerance in this forest, which is in a region (eastern North America) represented by only two studies in the global review of (Bennett *et al.*, 2015). We also test for an influence of potential access to available soil water, which should be greater for larger trees in dry but not in consistently wet microsites. Finally, we focus on the role of species' traits, testing the hypothesis that species' traits-–particularly leaf drought tolerance traits-–predict drought tolerance. We test predictions that drought tolerance is higher in ring-porous than semi-ring and diffuse-porous species and that it is correlated with wood density–either positively (Greenwood *et al.*, 2017) or negatively (Hoffmann *et al.*, 2011) and positively correlated with LMA. We further test predictions that species with low PLA_{dry} and those whose leaves lose turgor at lower water potentials (more negative π_{tlp}) have higher tolerance.

Materials and Methods

Study site and microclimate

Research was conducted at the 25.6-ha ForestGEO (Forest Global Earth Observatory) study plot at the Smithsonian Conservation Biology Institute (SCBI) in Virginia, USA (38°53'36.6"N, 78°08'43.4"W, elevation 273-338 m.a.s.l.; Fig. **S1**) (Bourg *et al.*, 2013; Anderson-Teixeira *et al.*, 2015a). Climate is humid temperate, with mean annual temperature of 12.7°C and precipitation of 1005 mm yr^{-1} during our study period (1960-2009; source: CRU TS v.4.01; Harris *et al.*, 2014). Dominant tree taxa within this secondary forest include *Liriodendron tulipifera*, oaks (*Quercus* spp.), and hickories (*Carya* spp.; Table 2).

Identifying drought years

We identified the three largest droughts within the time period 1960-2009, defining drought (Slette *et al.*, 2019) based on Palmer Drought Severity Index (PDSI) during May-August (MJJA; Table S1), which were identified by Helcoski *et al.* (2019) as the months to which annual tree growth was most sensitive at this site. PDSI divisional data for Northern Virginia were obtained in December 2017 from NOAA (https://www7.ncdc.noaa.gov/CDO/CDODivisionalSelect.jsp), from which we determined the three strongest droughts during the study period occurred in 1966, 1977, and 1999 (Figs. **1, S1**; Table S1).

The droughts differed in intensity and antecedent moisture conditions (Fig. **S1**, Table S1). The 1966 drought was preceded by two years of moderate drought during the growing season and severe to extreme drought starting the previous fall. In August 1966, $PDSI$ reached its lowest monthly value (-4.82) of the three droughts. The 1977 drought was the least intense throughout the growing season, and it was preceded by 2.5 years of near-normal conditions, making it the mildest of the three droughts. The 1999 drought was preceded by wetter than average conditions until the previous June, but $PDSI$ plummeted below -3.0 in October 1998 and remained below this threshold through August 1999. Following all three droughts, $PDSI$ rebounded to near-normal conditions in September or October (Fig. **S1**).

Data collection and preparation

Within or just outside the ForestGEO plot, we collected data on a suite of variables including tree heights, microenvironment characteristics, and species traits (Table 3). The SCBI ForestGEO plot was censused in 2008, 2013, and 2018 following standard ForestGEO protocols, whereby all free-standing woody stems $\geq$ 1cm diameter at breast height (DBH) were mapped, tagged, measured at DBH, and identified to species (Condit, 1998). From these census data, we used measurements of DBH from 2008 to calculate historical DBH and data for all stems $\geq$ 10cm to analyze functional trait composition relative to tree height (all analyses described below).

We analyzed tree-ring data (xylem growth increment) from 571 trees representing the twelve dominant species (Table 2; Fig. **S2**). Selected species were those with the greatest contributions to woody aboveground net primary productivity ($ANPP_{stem}$) and together comprised 97% of study plot $ANPP_{stem}$ between 2008 and 2013 (Helcoski *et al.*, 2019). Cores (one per tree) were collected within the ForestGEO plot at breast height (1.3m) in 2010-2011 or 2016-2017. In 2010-2011, cores were collected from randomly selected live trees of each species that had at least 30 individuals $\geq$ 10 cm DBH (Bourg *et al.*, 2013). In summers of 2016 and 2017, cores were collected from all trees found to have died within the preceding year based on annual tree mortality censuses (Gonzalez-Akre *et al.*, 2016). It is unlikely that drought was a factor in the death of any of these trees, as monthly May-Aug $PDSI$ did not drop below -1.75 (near-normal) in these years or the three years prior (2013-2017). Moreover, the trees analyzed here lived at least 17-18 years past the most recent major drought (1999), whereas the meta-analysis of Trugman *et al.* (2018) indicates that >10-year lags in drought-attributed mortality are rare. Having found that trees cored dead displayed similar climate sensitivity to trees cored live (Helcoski *et al.*, 2019), we pooled the samples for this analysis. Cores were sanded, measured, and crossdated using standard procedures, as detailed in (Helcoski *et al.*, 2019). The resulting chronologies (Fig. **1a**) were published in Zenodo (Gonzalez-Akre *et al.*, 2019).

For each cored tree, we combined tree-ring records and allometric equations of bark thickness to reconstruct DBH for the years 1950-2009. Prior DBH was estimated using the following equation:

$$DBH_Y = DBH_{2008} - 2 * \left[r_{bark,2008} - r_{bark,Y} + \sum_{year=Y}^{2008} r_{ring,Y} \right]$$

Here, Y denotes the year of interest, r_{ring} denotes ring width derived from cores, and r_{bark} denotes bark thickness, which was estimated from species-specific allometries based on the bark thickness data from the site (Table S2; Anderson-Teixeira *et al.*, 2015b).

Tree heights (H) were measured by several researchers for a variety of purposes between 2012 and 2019 (n=1,518 trees). Methods included direct measurements using a collapsible measurement rod on small trees (NEON, 2018) or a tape measure on recently fallen trees (this study); geometric calculations using clinometer and tape measure (Stovall *et al.*, 2018b) or digital rangefinders (Anderson-Teixeira *et al.*, 2015b; NEON, 2018); and ground-based LiDAR (Stovall *et al.*, 2018a). Rangefinders used either the tangent method (Impulse 200LR, TruPulse 360R) or the sine method (Nikon ForestryPro) for calculating heights. Both methods are associated with some error (Larjavaara & Muller-Landau, 2013), but in this instance there was no clear advantage of one or the other. Species-specific height allometries were developed using log-log regression ($ln[H] \sim ln[DBH]$; Table S3). For species with insufficient height data to create reliable species-specific allometries (n=2, *Juglans nigra* (JUNI) and *Fraxinus americana* (FRAM)), heights were calculated from an equation developed by combining the height measurements across all species. We then

used these allometries to estimate H for each drought year, Y, based on reconstructed DBH_Y (Fig. **S3**).

To characterize how environmental conditions vary with height, data were obtained from the NEON tower located <1km from the study area via the neonUtilities package (Lunch *et al.*, 2020). We used wind speed, relative humidity, and air temperature data, all measured over a vertical profile spanning heights from 7.2 m to above the top of the tree canopy (31.0 or 51.8m, depending on censor), for the years 2016-2018 (NEON, 2018). After filtering for missing and outlier values, we determined the daily minima and maxima, which we then aggregated at the monthly scale.

Crown position–a categorical variable classifying trees based on exposure to sunlight–was recorded for all cored trees that remained standing during the growing season of 2018 following the protocol of Jennings *et al.* (1999). Trees were classified as follows: *dominant* trees were defined as those with crowns above the general level of the canopy, *co-dominant* trees as those with crowns within the the canopy; *intermediate* trees as those with crowns below the canopy level, but illuminated from above; and *suppressed* as those below the canopy and receiving minimal direct illumination from above.

Topographic wetness index (TWI), used here as a metric of long-term mean moisture availability, was calculated using the dynatopmodel package in R (Fig. **S2**) (Metcalfe *et al.*, 2018). Originally developed by Beven & Kirkby (1979), TWI was part of a hydrological run-off model and has since been used for a number of purposes in hydrology and ecology (Sørensen *et al.*, 2006). TWI calculation depends on an input of a digital elevation model [DEM; ~3.7 m resolution from the elevatr package (Hollister, 2018), and from this yields a quantitative assessment defined by how "wet" an area is, based on areas where run-off is more likely. From our observations in the plot, TWI performed better at categorizing wet areas than the Euclidean distance from the stream.

Species' trait data were collected in August 2018 (Tables 2-3; Fig. **S4**). We sampled small, sun-exposed branches up to eight meters above the ground from three individuals of each species in and around the ForestGEO plot. Sampled branches were re-cut under water at least two nodes above the original cut and re-hydrated overnight in covered buckets under opaque plastic bags before measurements were taken. Rehydrated leaves taken towards the apical end of the branch (n=3 per individual: small, medium, and large) were scanned, weighed, dried at 60° C for $\geq$ 48 hours, and then re-scanned and weighed. Leaf area was calculated from scanned images using the LeafArea R package (Katabuchi, 2019). LMA was calculated as the ratio of leaf dry mass to fresh area. PLA_{dry} was calculated as the percent loss of area between fresh and dry leaves. WD was calculated for ~1cm diameter stem samples (bark and pith removed) as the ratio of dry weight to fresh volume, which was estimated using Archimedes' displacement. We used the rapid determination method of Bartlett *et al.* (2012) to estimate osmotic potential at turgor loss point (π_{tlp}). Briefly, two 4 mm diameter leaf discs were cut from each leaf, tightly wrapped in foil, submerged in liquid nitrogen, perforated 10-15 times with a dissection needle, and then measured using a vapor pressure osmometer (VAPRO 5520, Wescor, Logan, UT, USA). Osmotic potential (π_{osm}) given by the osmometer was used to estimate (π_{tlp}) using the equation $\pi_{tlp} = 0.832\pi_{osm}^{-0.631}$ (Bartlett *et al.*, 2012).

Statistical Analysis

For each drought year, we calculated metrics of drought resistance (Rt), recovery (Rc), and resilience (Rs), following Lloret *et al.* (2011). These metrics compare ratios of basal area increment (BAI; *i.e.*, change in cross-sectional area) before, during, and after the drought year, as specified in Table 3.
For all metrics, values <1 and >1 indicate growth reductions and increases, respectively.

Because these metrics could potentially be biased by directional pre-drought growth trends, we also tried an intervention time series analysis (ARIMA, Hyndman *et al.*, 2020) that predicted mean drought-year growth based on trends over the preceding ten years and used this value in place of the five-year mean in calculations of resistance (Rt_{ARIMA}= observed BAI/ predicted BAI). Rt and Rt_{ARIMA} were strongly correlated (Fig. **S5**), and showed similar responses to the independent variables of interest (cf. Tables S4-55, S8-S9). Visual review of the individual tree-ring sequences with the largest discrepancies between these metrics revealed that Rt was less prone to unreasonable estimates than Rt_{ARIMA}. We therefore determined that use of 5-year means, as described above, were more appropriate metrics than those based on ARIMA projections.

Analyses focused on testing the predictions presented in Table 1 with Rt (or Rt_{ARIMA}), Rc, or Rs as the response variable. Models were run for all drought years combined and for each drought year individually. The general statistical model for hypothesis testing was a mixed effects model, implemented in the lme4 package in R (Bates *et al.*, 2019). In the multi-year model, we included a random effect of tree nested within species and a fixed effect of drought year to represent the combined effects of differences in drought characteristics. Individual year models included a random effect of species. All models included fixed effects of independent variables of interest (Tables 1,3) as specified below. All variables across all best models had variance inflation factors between 1 and 1.045. We used Akaike information criterion with correction for small sample sizes (AICc; see Brewer *et al.*, 2016) to assess model selection, and conditional/marginal R-squared to assess model fit as implemented in the AICcmodavg package in R (Mazerolle & Dan Linden., 2019). Individual model terms were considered significant when their addition to a model improved fit at ΔAICc $\geq$ 2.0, where ΔAICc is the difference in AICc between models with and without the trait.

To avoid over-fitting models with five species traits (Table 3) across only 12 species, we did not include all traits as fixed effects in a single linear mixed model, but rather conducted individual tests of each species trait to determine the relative importance and appropriateness for inclusion in the main model. These tests followed the model structure specified above, with $ln[H]$ and $ln[TWI]$ added to create a base model against which we tested traits. Trait variables were considered appropriate for inclusion in the main model if their addition to the base model significantly improved fit for at least one metric of drought tolerance (Rt, Rc, or Rs; Tables S4,S6-S7). Although we tested xylem porosity as a predictor (Table 1), we did not consider it appropriate for inclusion in the main model because of its highly uneven distribution of species across categories (Table 2). In addition, we observed opposite drought responses of the only two diffuse-porous species (see Results), themselves likely representing the most and least shade-tolerant species in the study area.

We then determined the top full models for predicting each dependent variable. To do so, we compared models with all possible combinations of candidate variables, including $ln[H]$*$ln[TWI]$ and species traits as specified above. We identified the full set of models within ΔAICc=2 of the best model (that with lowest AICc). When a variable appeared in all of these models and the sign of the coefficient was consistent across models, we viewed this as support for the acceptance/rejection of the associated prediction (Table 1). If the variable appeared in some but not all of these models, and its sign was consistent across models, we considered this partial support/rejection.

All analysis beyond basic data collection was performed using R version 3.6.2 (R Core Team, 2019). Other R-packages used in analyses are listed in the Supplementary Information (Methods S1).

Results

Tree height and microenvironment

In the years for which we have vertical profiles in climate data (2016-2018), taller trees–or those in dominant crown positions– were generally exposed to higher evaporative demand during the peak growing season months (May-August; Fig. **2**). Specifically, maximum daily wind speeds were significantly higher above the top of the canopy (40-50m) than within and below (10-30m) (Fig. **2a**). Relative humidity was also somewhat lower during June-August, ranging from ~50-80% above the canopy and ~60-90% in the understory (Fig. **2b**). Air temperature did not vary consistently across the vertical profile (Fig. **2c**).

Crown position varied as expected with height (dominant > co-dominant > intermediate > suppressed), but with substantial variation (Fig. **2d**). There were significant differences in height across all crown position classes (Fig. **2d**). A comparison test between height and crown position data from the most recent ForestGEO census (2018) revealed a correlation of 0.73.

Community-level drought responses

At the community level, cored trees showed substantial growth reductions in all three droughts, with a mean Rt of 0.86 in 1966 and 1999, and 0.84 in 1977 (Fig. **1b**). Across the entire study period (1950-2009), the focal drought years were the three years with the largest fraction of trees exhibiting $Rt \leq 0.7$. Specifically, in each drought, roughly 30% of the cored trees had growth reductions of $\geq 30\%$ ($Rt \leq 0.7$): 29% in 1966, 32% in 1977, and 27% in 1999. However, some individuals exhibited increased growth, *i.e.*, $Rt > 1.0$: 26% of trees in 1966, 22% in 1977, and 26% in 1999. Recovery was generally strong and complete within five years following each of the drought years, with Rc averaging 1.55 in 1966, 1.42 in 1977, and 1.34 in 1999 (Fig. **S6**) and Rs averaging 1.28 in 1966, 1.19 in 1977, and 1.12 in 1999 (Fig. **1c**).

In the context of the multivariate models, all response variables varied across drought years. That is, in models with all drought years combined, year was present in all of the top models – *i.e.*, models that were statistically indistinguishable (ΔAICc<2) from the best model (see footnotes on Tables S8-S11). For Rt, differences among drought years were small (<0.02; Table S8). In contrast, differences among years were larger for Rc and Rs, with coefficients for year highest in 1966, intermediate in 1977, and lowest in 1999.

Tree height, microenvironment, and drought tolerance

Taller trees (based on H in the drought year) showed stronger growth reductions during drought (*i.e.*, lower Rt) and less rebound following drought (*i.e.*, lower Rc and Rs; Table 1; Fig. **4**). Specifically, for Rt, $ln[H]$ appeared, with negative coefficient, in the best model (ΔAICc=0) and all top models when evaluating the three drought years together (Tables S8-S9). The same held true for 1966 individually, but there was no significant effect of $ln[H]$ for 1977 or 1999 individually. For Rc, $ln[H]$ appeared, with negative coefficient, in the best model without a $ln[H] * ln[TWI]$ interaction, for the three drought years together and for 1977, but not for 1966 or 1999. For Rs, again considering the best models without a $ln[H] * ln[TWI]$ interaction, there was a negative effect of $ln[H]$ for the three drought years together and for 1966 and 1977, and a non-significant negative trend in 1999.

Trees in drier microsites showed greater growth declines during drought; *i.e.*, Rt had a significantly negative response to $ln[TWI]$ across all drought years combined, and in 1977 and 1999 individually (Fig. **4**, Table S8-S9). The $ln[H] * ln[TWI]$ interaction was never significant, and had a positive sign in any top Rt models in which it appeared (Tables 1, S8-S9), rejecting the hypothesis that smaller trees (presumably with smaller

rooting volume) are more susceptible to drought in microenvironments with a deeper water table. In contrast, $ln[TWI]$ did not appear in any of the best models for Rc or Rs (combined of for individual years), except in interaction with $ln[H]$ (Fig. **4**, Tables S10-S11). Negative $ln[H] * ln[TWI]$ interactions appeared in the best models for both Rc and Rs for all years combined, as well as in one individual year for each (1966 for Rc, 1977 for Rs). This implies a non-significant tendency for small trees to have greater recovery and resilience in wetter microhabitats, but for large trees to have greater recovery and resilience in dry microhabitats.

Species' traits and drought tolerance

Species, as a factor in ANOVA, had significant ($p<0.05$) influence on all traits (WD, LMA, PLA_{dry}, and π_{tlp}), with more significant pairwise differences for WD and PLA_{dry} than for LMA and π_{tlp} (Table 2, Fig. **S4**). Drought tolerance also varied across species, overall and in each drought year (Figs. **3, S7**). Species with overall lowest and highest Rt and Rs were, respectively, *L. tulipifera* (mean $Rt = 0.66$, mean $Rs = 1.04$) and *Fagus grandifolia* (mean $Rt = 0.99$; mean $Rs = 1.65$). These two species–notably the only two diffuse-porous species in our study–differed significantly from one another in Rt and Rs in each drought year (Fig. **3**).

WD, LMA, and xylem porosity were all poor predictors of drought tolerance (Tables 1, S4-S5). WD and LMA were never significantly associated with Rt, Rc, or Rs in the single-variable tests and were therefore excluded from the full models. Xylem porosity had no significant influence on Rt or Rs in models for all droughts combined (Tables S4, S7). In contrast, Rc was significantly higher in diffuse- and semi-ring porous species than in ring-porous species (Table S6, Fig. **3**).

Drought resistance and resilience, but not recovery, were negatively correlated with PLA_{dry} and π_{tlp} (Fig. **4**; Tables 1, S4-S11). For Rt, PLA_{dry} had a significant influence, with negative coefficient, in top models for the three droughts combined and for the 1966 drought individually (Fig. **4**; Tables S8-S9). It was also included in some of the top models for 1999 (Tables S8-S9). π_{tlp} was included with a negative coefficient in the best model for the combined droughts scenario and for the 1977 drought individually (Fig. **4**; Table S8), although its influence was not significant at ΔAICc<2. It was also included in some of the top models for 1999 (Tables S8-S9).

Recovery was not significantly correlated with either PLA_{dry} or π_{tlp}. There was only one best Rc model containing one of these terms (π_{tlp} in 1977 drought), but in no instance was one of these terms included in all top models (i.e., at ΔAICc<2).

For Rs, PLA_{dry} was in the best models for the three droughts combined and for the 1966 drought individually, and some of the top models for 1977 and 1999 (Fig. **4**; Table S11); however, its effects were not significant at ΔAICc<2. π_{tlp} was in the best models for the three droughts combined and for 1966 and 1999 individually, and in one of the top models for 1977 (Fig. **4**; Table S11). However, its effects were significant at ΔAICc<2 for 1999 only.

Discussion

Tree height, microenvironment, and leaf drought tolerance traits shaped tree growth responses across three droughts at our study site (Table 1, Fig. **4**). Taller trees had greater exposure to conditions that would promote water loss and heat damage during drought (Fig. **2**), which is one plausible mechanism for their lower drought resistance, recovery, and resilience (Fig. **4**). There was no evidence that greater availability of,

or access to, soil water availability increased drought resistance; in contrast, trees in wetter topographic positions had lower Rt (Zuleta *et al.*, 2017; Stovall *et al.*, 2019), and the larger potential rooting volume of large trees provided no advantage in the drier microenvironments. The negative effect of height on Rt held after accounting for species' traits, which is consistent with recent work finding height had a stronger influence on mortality risk than forest type during drought (Stovall *et al.*, 2020). Drought tolerance was not consistently linked to species' LMA, WD, or xylem type (ring- vs. diffuse porous), but was negatively correlated with leaf drought tolerance traits (PLA_{dry}, π_{tlp}). This is the first study to our knowledge linking PLA_{dry} and π_{tlp} to growth reduction during drought. The directions of these responses were consistent across droughts (Table S8), supporting the premise that they were driven by fundamental physiological mechanisms. However, the strengths of each predictor varied across droughts (Fig. **4**; Tables S8-S9), indicating that drought characteristics interact with tree size, microenvironment, and traits to shape which individuals are most affected. These findings advance our knowledge of the factors that make trees vulnerable to stem growth declines during drought and, by extension, likely make them more vulnerable to mortality (Sapes *et al.*, 2019).

The droughts considered here were of a magnitude that has occurred with an average frequency of approximately once every 10-15 years (Fig. **1a**, Helcoski *et al.*, 2019) and had substantial but short-lived impacts on tree growth (Fig. **1**). These droughts were classified as severe ($PDSI <$ -3.0; 1977) or extreme ($PDSI <$ -4.0; 1966, 1999) at our site and have been linked to tree mortality in the eastern United States (Druckenbrod *et al.*, 2019), but were modest compared to the so-called "megadroughts" that have triggered massive tree die-off in other regions (e.g., Allen *et al.*, 2010; Clark *et al.*, 2016; Stovall *et al.*, 2019). Of the droughts considered here, the 1966 drought, which was preceded by two years of dry conditions (Fig. **S1**), severely stressed a larger portion of trees (Fig. **1b**). The tendency for large trees to have lowest resistance was most pronounced in this drought, consistent with other findings that this physiological response increases with drought severity (Bennett *et al.*, 2015; Stovall *et al.*, 2019). Across all three droughts, the majority of trees experienced reduced growth, but a substantial portion (e.g., short understory trees, species with drought resistant traits) had increased growth (Figs. **1b, 4**), consistent with prior observations that smaller trees can exhibit increased growth rates during drought (Bennett *et al.*, 2015). Growth rebounded strongly following the droughts, on average exceeding pre-drought growth rates (Fig. **1**), particularly for shorter trees and species with drought-tolerant traits (Figs. **3-4**). It is likely because of the moderate impact of these droughts, along with other factors influencing tree growth (e.g., stand dynamics), that our best models characterize only a modest amount of variation in Rt, Rc, and Rs: 11-18% for all droughts combined, and 13-30% for individual droughts (Tables S8-S11).

Consistent with studies in other forests worldwide (Bennett *et al.*, 2015), taller trees in this forest exhibited lower drought resistance–and also recovery and resilience–when compared to smaller trees. Mechanistically, this is consistent with, and reinforces, previous findings for a trade-off between the ability of trees to efficiently transport water to great heights and simultaneously maintain strong resistance and resilience to drought-induced embolism (Couvreur *et al.*, 2018; Roskilly *et al.*, 2019; Olson *et al.*, 2018; Liu *et al.*, 2019). Taller trees also face dramatically distinctive microenvironments (Fig. **2**). They are exposed to higher wind speeds and lower humidity (Fig. **2a,b**), resulting in higher evaporative demand. Unlike other temperate forests where modestly cooler understory conditions have been documented (Zellweger *et al.*, 2019), particularly under drier conditions (Davis *et al.*, 2019), we observed no significant variation in air temperatures across the vertical profile (Fig. **2c**). More critically for tree physiology, leaf temperatures can

become significantly elevated over air temperature under conditions of high solar radiation and low stomatal conductance (Campbell & Norman, 1998; Rey-Sánchez *et al.*, 2016). Under drought, when direct solar radiation tends to be higher (because of less cloud cover) and less water is available for evaporative cooling of the leaves, trees with sun-exposed crowns may not be able to simultaneously maintain leaf temperatures below damaging extremes and avoid drought-induced embolism. Indeed, previous studies have shown lower drought resistance in more exposed trees (Liu & Muller, 1993; Suarez *et al.*, 2004; Scharnweber *et al.*, 2019). Unfortunately, collinearity between height and crown exposure in this study (Fig. **2d**) makes it impossible to confidently partition causality. Additional research comparing drought responses of early successional and mature forest stands, along with short and tall isolated trees, would be valuable for more clearly disentangling the roles of tree height and crown exposure.

Belowground, taller trees would tend to have larger root systems (Enquist & Niklas, 2002; Hui *et al.*, 2014), but this does not necessarily imply that they have greater access to or reliance on deep soil-water resources that may be critical during drought. While tree size can correlate with the depth of water extraction (Brum *et al.*, 2019), the linkage is not consistent. Shorter trees can vary broadly in the depth of water uptake (Stahl *et al.*, 2013), and larger trees may allocate more to abundant shallow roots that are beneficial for taking up water from rainstorms (Meinzer *et al.*, 1999). Moreover, reliance on deep soil-water resources can actually prove a liability during severe and prolonged drought, as these can experience more intense water scarcity relative to non-drought conditions (Chitra-Tarak *et al.*, 2018). In any case, the potentially greater access to water did not override the disadvantage conferred by height–and, in fact, greater moisture access in non-drought years (here, higher TWI) appears to make trees more sensitive to drought (Zuleta *et al.*, 2017; Stovall *et al.*, 2019). This may be because moister habitats would tend to support species and individuals with more mesophytic traits (Mencuccini, 2003; Bartlett *et al.*, 2016b; Medeiros *et al.*, 2019), potentially growing to greater heights (e.g., Detto *et al.*, 2013), and these are then more vulnerable when drought occurs. The observed height-sensitivity of Rt, together with the lack of conferred advantage to large stature in drier topographic positions, agrees with the concept that physiological limitations to transpiration under drought shift from soil water availability to the plant-atmosphere interface as forests age (Bretfeld *et al.*, 2018), such that tall, dominant trees are the most sensitive in mature forests. Again, additional research comparing drought responses across forests with different tree heights and water availability would be valuable for disentangling the relative importance of above- and belowground mechanisms across trees of different size.

The development of tree-ring chronologies for the twelve most dominant tree species at our site (Bourg *et al.*, 2013; Helcoski *et al.*, 2019) provided a sufficient sample size to compare historical drought responses across species (Fig. **3**) and associated traits at a single site (see also Elliott *et al.*, 2015). Our study reinforced current understanding (see Introduction) that WD and LMA are not reliably linked to drought tolerance (Table 1). Contrary to several previous studies in temperate deciduous forests (Kannenberg *et al.*, 2019; Friedrichs *et al.*, 2009; Elliott *et al.*, 2015), we did not find an association between xylem porosity and drought resistance or resilience, as the two diffuse-porous species, *L.* and *F. grandifolia*, were at opposite ends of the Rt spectrum (Fig. **3**). While the low Rt of *L. tulipifera* is consistent with other studies (Elliott *et al.*, 2015), the high Rt of *F. grandifolia* contrasts with studies identifying diffuse porous species in general (Kannenberg *et al.*, 2019; Elliott *et al.*, 2015), and the genus *Fagus* in particular (Friedrichs *et al.*, 2009), as drought sensitive. There are two potential explanations for this discrepancy. First, other traits can and do override the influence of xylem porosity on drought resistance. Ring-porous species are restricted mainly to temperate deciduous forests, while highly drought-tolerant diffuse-porous species exist in other biomes

(Wheeler *et al.*, 2007). *F. grandifolia* had intermediate π_{tlp} and low PLA_{dry} (Fig. **S4**), which would have contributed to its drought tolerance (Fig. **4**; see discussion below), in concordance with studies identifying *Fagus* species as intermediate in drought tolerance (Vitasse *et al.*, 2019; Pretzsch *et al.*, 2018). A second explanation of why *F. grandifolia* trees at this particular site had higher Rt and Rs is that the sampled individuals, reflective of the population within the plot, are generally shorter and in less-dominant canopy positions compared to most other species (Fig. **S4**). The species, which is highly shade-tolerant, also has deep crowns (Anderson-Teixeira *et al.*, 2015b), implying that a lower proportion of leaves would be affected by harsher microclimatic conditions at the top of the canopy under drought (Fig. **2**). Thus, the high Rt and Rs of the sampled *F. grandifolia* population can be explained by a combination of fairly drought-resistant leaf traits, shorter stature, and a buffered microenvironment.

Concerted measurement of tree-rings and leaf drought tolerance traits of emerging importance in published literature (Medeiros *et al.*, 2019; Scoffoni *et al.*, 2014; Bartlett *et al.*, 2016a) allowed novel insights into the role of drought tolerance traits in shaping drought response. The finding that PLA_{dry} and π_{tlp} can be useful for predicting drought responses of tree growth (Fig. **4**; Table 1) is both novel and consistent with previous studies linking these traits to habitat and drought tolerance. Previous studies have demonstrated that π_{tlp} and PLA_{dry} are physiologically meaningful traits linked to species distribution along moisture gradients (Maréchaux *et al.*, 2015; Fletcher *et al.*, 2018; Medeiros *et al.*, 2019; Rosas *et al.*, 2019; Simeone *et al.*, 2019; Zhu *et al.*, 2018), and our findings indicate that these traits also influence drought responses. Furthermore, the observed linkage of π_{tlp} to Rt in this forest aligns with observations in the Amazon that π_{tlp} is higher in drought-intolerant than drought-tolerant plant functional type. Further, it adds support to the idea that this trait is useful for categorizing and representing species' drought responses in models (Powell *et al.*, 2017). Because both PLA_{dry} and π_{tlp} can be measured relatively easily (Bartlett *et al.*, 2012; Scoffoni *et al.*, 2014), they hold promise for predicting drought growth responses across diverse forests. The importance of predicting drought responses from species traits increases with tree species diversity; whereas it is feasible to study drought responses for all dominant species in most boreal and temperate forests (e.g., this study), this becomes difficult to impossible for diverse tropical forests where most species do not form annual rings (but see Schöngart *et al.*, 2017 for a review of progress in tropical dendroecology). A full linkage of drought tolerance traits to drought responses would be invaluable for forecasting how little-known species and whole forests will respond to future droughts (Powell *et al.*, 2017; Christoffersen *et al.*, 2016).

As climate change drives increasing drought in many of the world's forests (Intergovernmental Panel on Climate Change, 2015; Trenberth *et al.*, 2014), the fate of forests and their climate feedbacks will be shaped by the biophysical and physiological drivers observed here. Our results show that taller, more exposed trees and species with less drought-tolerant leaf traits will be most affected in terms of both growth during the drought year and subsequent growth. Survival is linked to resistance and resilience (DeSoto *et al.*, 2020; Gessler *et al.*, 2020), implying it may be influenced by the same factors. Indeed, while no link between PLA_{dry} or π_{tlp} on drought survival has been established (but see Powers *et al.*, 2020), taller trees have lower survival (Bennett *et al.*, 2015; Stovall *et al.*, 2019). As climate change-driven droughts affect forests worldwide, there is likely to be a shift from mature forests with tall, buffering trees to forests with a shorter overall stature (McDowell *et al.*, 2020). At this point, species whose drought tolerance relies in part on existence within a buffered microenvironment (e.g., *F. grandifolia*) could in turn become more susceptible. Here, the relative importance of tree height *per se* versus crown exposure becomes crucial, shaping whether the dominant trees of shorter canopies are significantly more drought tolerant because of their shorter

stature, or whether high exposure makes them as vulnerable as the taller trees of the former canopy. Studies disentangling the influence of height and exposure on drought tolerance will be critical to answering this question. Ultimately, distributions of tree heights and drought tolerance traits across broad moisture gradients suggest that forests exposed to more drought will shift towards shorter stature and be dominated by species with more drought-tolerant traits (Bartlett *et al.*, 2016a; Zhu *et al.*, 2018; Liu *et al.*, 2019). Our study helps to elucidate the mechanisms behind these patterns, opening the door for more accurate forecasting of forest responses to future drought.

Acknowledgements

We especially thank the numerous researchers who helped to collect the data used here, in particular Jennifer C. McGarvey, Jonathan R. Thompson, and Victoria Meakem for original collection and processing of cores. Thanks also to Camila D. Medeiros for guidance on leaf drought tolerance and functional trait measurements, Edward Brzostek's lab for collaboration on leaf sampling, and Maya Prestipino for data collection. This manuscript was improved based on helpful reviews by Mark Olson and three anonymous reviewers. Funding for the establishment of the SCBI ForestGEO Large Forest Dynamics Plot was provided by the Smithsonian-led Forest Global Earth Observatory (ForestGEO), the Smithsonian Institution, and the HSBC Climate Partnership. This study was funded by ForestGEO, a Virginia Native Plant Society grant to KAT and AJT, and support from the Harvard Forest and National Science Foundation which supports the PalEON project (NSF EF-1241930) for NP.

Author Contribution

KAT, IM, and AJT designed the research. Tree-ring chronologies were developed by RH under guidance of AJT, KAT, and NP. Trait data were collected by IM and JZ under guidance of NK, KAT, and LS. Other plot data were collected by NB in coordination with WM and by IM and AS under guidance of EGA and KAT. Data analyses were performed by IM under guidance of KAT and VH. KAT and IM interpreted the results. IM and KAT wrote the first draft of manuscript, and all authors contributed to revisions.

Data and code availability

All data, code, and results are available through the SCBI-ForestGEO organization on GitHub (https://github.com/SCBI-ForestGEO: SCBI-ForestGEO-Data and McGregor_climate-sensitivity-variation repositories), with static versions corresponding to data and analyses presented here archived in Zenodo (DOIs: 10.5281/zenodo.3604993 and *[TBD]*, respectively. Full ForestGEO census data for SCBI are available through the ForestGEO data portal (www.forestgeo.si.edu).

ORCID

Ian R. McGregor: https://orcid.org/0000-0002-5763-021X

Kristina J. Anderson-Teixeira: https://orcid.org/0000-0001-8461-9713

Supplementary Information

Table S1. Monthly Palmer Drought Severity Index (PDSI), and its rank among all years between 1950 and 2009 for focal droughts.

References

Abrams MD. **1990**. Adaptations and responses to drought in Quercus species of North America. *Tree Physiology* **7**: 227–238.

Allen CD, Breshears DD, McDowell NG. **2015**. On underestimation of global vulnerability to tree mortality and forest die-off from hotter drought in the Anthropocene. *Ecosphere* **6**: art129.

Allen CD, Macalady AK, Chenchouni H, Bachelet D, McDowell N, Vennetier M, Kitzberger T, Rigling A, Breshears DD, Hogg EH(***et al.*** **2010**. A global overview of drought and heat-induced tree mortality reveals emerging climate change risks for forests. *Forest Ecology and Management* **259**: 660–684.

Anderegg WRL, Klein T, Bartlett M, Sack L, Pellegrini AFA, Choat B, Jansen S. **2016**. Meta-analysis reveals that hydraulic traits explain cross-species patterns of drought-induced tree mortality across the globe. *Proceedings of the National Academy of Sciences* **113**: 5024–5029.

Anderson-Teixeira KJ, Davies SJ, Bennett AC, Gonzalez-Akre EB, Muller-Landau HC, Wright SJ, Salim KA, Zambrano AMA, Alonso A, Baltzer JL ***et al.*** **2015a**. CTFS-ForestGEO: A worldwide network monitoring forests in an era of global change. *Global Change Biology* **21**: 528–549.

Anderson-Teixeira KJ, McGarvey JC, Muller-Landau HC, Park JY, Gonzalez-Akre EB, Herrmann V, Bennett AC, So CV, Bourg NA, Thompson JR ***et al.*** **2015b**. Size-related scaling of tree form and function in a mixed-age forest. *Functional Ecology* **29**: 1587–1602.

Bartlett MK, Klein T, Jansen S, Choat B, Sack L. **2016a**. The correlations and sequence of plant stomatal, hydraulic, and wilting responses to drought. *Proceedings of the National Academy of Sciences* **113**: 13098–13103.

Bartlett MK, Scoffoni C, Ardy R, Zhang Y, Sun S, Cao K, Sack L. **2012**. Rapid determination of comparative drought tolerance traits: Using an osmometer to predict turgor loss point. *Methods in Ecology and Evolution* **3**: 880–888.

Bartlett MK, Zhang Y, Yang J, Kreidler N, Sun S-W, Lin L, Hu Y-H, Cao K-F, Sack L. **2016b**. Drought tolerance as a driver of tropical forest assembly: Resolving spatial signatures for multiple processes. *Ecology* **97**: 503–514.

Bates D, Maechler M, Bolker B, Walker S. **2019**. *Lme4: Linear mixed-effects models using 'eigen' and s4.*

Bennett AC, McDowell NG, Allen CD, Anderson-Teixeira KJ. **2015**. Larger trees suffer most during drought in forests worldwide. *Nature Plants* **1**: 15139.

Beven KJ, Kirkby MJ. **1979**. A physically based, variable contributing area model of basin hydrology / Un modèle à base physique de zone d'appel variable de l'hydrologie du bassin versant. *Hydrological Sciences Bulletin* **24**: 43–69.

Bonan GB. **2008**. Forests and Climate Change: Forcings, Feedbacks, and the Climate Benefits of Forests. *Science* **320**: 1444–1449.

Bourg NA, McShea WJ, Thompson JR, McGarvey JC, Shen X. **2013**. Initial census, woody seedling, seed rain, and stand structure data for the SCBI SIGEO Large Forest Dynamics Plot. *Ecology* **94**: 2111–2112.

583 Bretfeld M, Ewers BE, Hall JS. **2018**. Plant water use responses along secondary forest succession during
584 the 2015–2016 El Niño drought in Panama. *New Phytologist* **219**: 885–899.

585 Brewer MJ, Butler A, Cooksley SL. **2016**. The relative performance of AIC, AICC and BIC in the presence
586 of unobserved heterogeneity. *Methods in Ecology and Evolution* **7**: 679–692.

587 Brum M, Vadeboncoeur MA, Ivanov V, Asbjornsen H, Saleska S, Alves LF, Penha D, Dias JD, Aragão
588 LEOC, Barros F ***et al.*** **2019**. Hydrological niche segregation defines forest structure and drought tolerance
589 strategies in a seasonal Amazon forest. *Journal of Ecology* **107**: 318–333.

590 Campbell GS, Norman JM. **1998**. *An Introduction to Environmental Biophysics*. New York: Springer.

591 Chitra-Tarak R, Ruiz L, Dattaraja HS, Kumar MSM, Riotte J, Suresh HS, McMahon SM, Sukumar R.
592 **2018**. The roots of the drought: Hydrology and water uptake strategies mediate forest-wide demographic
593 response to precipitation. *Journal of Ecology* **106**: 1495–1507.

594 Christoffersen BO, Gloor M, Fauset S, Fyllas NM, Galbraith DR, Baker TR, Kruijt B, Rowland L, Fisher
595 RA, Binks OJ ***et al.*** **2016**. Linking hydraulic traits to tropical forest function in a size-structured and
596 trait-driven model (TFS v.1-Hydro).

597 Clark JS, Iverson L, Woodall CW, Allen CD, Bell DM, Bragg DC, D'Amato AW, Davis FW, Hersh MH,
598 Ibanez I ***et al.*** **2016**. The impacts of increasing drought on forest dynamics, structure, and biodiversity in
599 the United States. *Global Change Biology* **22**: 2329–2352.

600 Condit R. **1998**. *Tropical Forest Census Plots: Methods and Results from Barro Colorado Island, Panama*
601 *and a Comparison with Other Plots*. Berlin, Heidelberg: Springer Berlin Heidelberg.

602 Cook BI, Ault TR, Smerdon JE. **2015**. Unprecedented 21st century drought risk in the American Southwest
603 and Central Plains. *Science Advances* **1**: e1400082.

604 Couvreur V, Ledder G, Manzoni S, Way DA, Muller EB, Russo SE. **2018**. Water transport through tall
605 trees: A vertically explicit, analytical model of xylem hydraulic conductance in stems. *Plant, Cell &*
606 *Environment* **41**: 1821–1839.

607 Dai A, Zhao T, Chen J. **2018**. Climate Change and Drought: A Precipitation and Evaporation Perspective.
608 *Current Climate Change Reports* **4**: 301–312.

609 Davis KT, Dobrowski SZ, Holden ZA, Higuera PE, Abatzoglou JT. **2019**. Microclimatic buffering in forests
610 of the future: The role of local water balance. *Ecography* **42**: 1–11.

611 DeSoto L, Cailleret M, Sterck F, Jansen S, Kramer K, Robert EMR, Aakala T, Amoroso MM, Bigler C,
612 Camarero JJ ***et al.*** **2020**. Low growth resilience to drought is related to future mortality risk in trees.
613 *Nature Communications* **11**: 545.

614 Detto M, Muller-Landau HC, Mascaro J, Asner GP. **2013**. Hydrological Networks and Associated
615 Topographic Variation as Templates for the Spatial Organization of Tropical Forest Vegetation. *PLOS ONE*
616 **8**: e76296.

617 Druckenbrod DL, Martin-Benito D, Orwig DA, Pederson N, Poulter B, Renwick KM, Shugart HH. **2019**.
618 Redefining temperate forest responses to climate and disturbance in the eastern United States: New insights
619 at the mesoscale. *Global Ecology and Biogeography* **28**: 557–575.

Elliott KJ, Miniat CF, Pederson N, Laseter SH. **2015**. Forest tree growth response to hydroclimate variability in the southern Appalachians. *Global Change Biology* **21**: 4627–4641.

Enquist BJ, Niklas KJ. **2002**. Global Allocation Rules for Patterns of Biomass Partitioning in Seed Plants. *Science* **295**: 1517–1520.

Farrell C, Szota C, Arndt SK. **2017**. Does the turgor loss point characterize drought response in dryland plants? *Plant, Cell & Environment* **40**: 1500–1511.

Fletcher LR, Cui H, Callahan H, Scoffoni C, John GP, Bartlett MK, Burge DO, Sack L. **2018**. Evolution of leaf structure and drought tolerance in species of Californian Ceanothus. *American Journal of Botany* **105**: 1672–1687.

Friedlingstein P, Cox P, Betts R, Bopp L, Bloh W von, Brovkin V, Cadule P, Doney S, Eby M, Fung I ***et al.*** **2006**. Climate–Carbon Cycle Feedback Analysis: Results from the C4MIP Model Intercomparison. *Journal of Climate* **19**: 3337–3353.

Friedrichs DA, Trouet V, Büntgen U, Frank DC, Esper J, Neuwirth B, Löffler J. **2009**. Species-specific climate sensitivity of tree growth in Central-West Germany. *Trees* **23**: 729.

Gessler A, Bottero A, Marshall J, Arend M. **2020**. The way back: Recovery of trees from drought and its implication for acclimation. *New Phytologist*.

Gillerot L, Forrester DI, Bottero A, Rigling A, Lévesque M. **2020**. Tree Neighbourhood Diversity Has Negligible Effects on Drought Resilience of European Beech, Silver Fir and Norway Spruce. *Ecosystems*.

Gonzalez-Akre E, Anderson-Teixeira K, McGregor I, Herrmann V, RHelcoski. **2019**. SCBI-ForestGEO/SCBI-ForestGEO-Data: First official release.

Gonzalez-Akre E, Meakem V, Eng C-Y, Tepley AJ, Bourg NA, McShea W, Davies SJ, Anderson-Teixeira K. **2016**. Patterns of tree mortality in a temperate deciduous forest derived from a large forest dynamics plot. *Ecosphere* **7**: e01595.

Greenwood S, Ruiz-Benito P, Martínez-Vilalta J, Lloret F, Kitzberger T, Allen CD, Fensham R, Laughlin DC, Kattge J, Bönisch G ***et al.*** **2017**. Tree mortality across biomes is promoted by drought intensity, lower wood density and higher specific leaf area. *Ecology Letters* **20**: 539–553.

Guerfel M, Baccouri O, Boujnah D, Chaïbi W, Zarrouk M. **2009**. Impacts of water stress on gas exchange, water relations, chlorophyll content and leaf structure in the two main Tunisian olive (Olea europaea L.) Cultivars. *Scientia Horticulturae* **119**: 257–263.

Harris I, Jones PD, Osborn TJ, Lister DH. **2014**. Updated high-resolution grids of monthly climatic observations – the CRU TS3.10 Dataset. *International Journal of Climatology* **34**: 623–642.

Helcoski R, Tepley AJ, Pederson N, McGarvey JC, Meakem V, Herrmann V, Thompson JR, Anderson-Teixeira KJ. **2019**. Growing season moisture drives interannual variation in woody productivity of a temperate deciduous forest. *New Phytologist* **0**.

Hoffmann WA, Marchin RM, Abit P, Lau OL. **2011**. Hydraulic failure and tree dieback are associated with high wood density in a temperate forest under extreme drought. *Global Change Biology* **17**: 2731–2742.

Hollister J. **2018**. *Elevatr: Access elevation data from various apis*.

Hui D, Wang J, Shen W, Le X, Ganter P, Ren H. **2014**. Near Isometric Biomass Partitioning in Forest Ecosystems of China. *PLOS ONE* **9**: e86550.

Hyndman R, Athanasopoulos G, Bergmeir C, Caceres G, Chhay L, O'Hara-Wild M, Petropoulos F, Razbash S, Wang E, Yasmeen F. **2020**. *Forecast: Forecasting functions for time series and linear models.*

Intergovernmental Panel on Climate Change. **2015**. *Climate Change 2014: Impacts, Adaptation and Vulnerability: Working Group II Contribution to the IPCC Fifth Assessment Report. Volume 2 Volume 2.*

Jennings SB, Brown ND, Sheil D. **1999**. Assessing forest canopies and understorey illumination: Canopy closure, canopy cover and other measures. *Forestry: An International Journal of Forest Research* **72**: 59–74.

Kannenberg SA, Novick KA, Alexander MR, Maxwell JT, Moore DJP, Phillips RP, Anderegg WRL. **2019**. Linking drought legacy effects across scales: From leaves to tree rings to ecosystems. *Global Change Biology* **0**.

Katabuchi M. **2019**. *LeafArea: Rapid digital image analysis of leaf area.*

Kennedy D, Swenson S, Oleson KW, Lawrence DM, Fisher R, Costa ACL da, Gentine P. **2019**. Implementing Plant Hydraulics in the Community Land Model, Version 5. *Journal of Advances in Modeling Earth Systems* **11**: 485–513.

Koike T, Kitao M, Maruyama Y, Mori S, Lei TT. **2001**. Leaf morphology and photosynthetic adjustments among deciduous broad-leaved trees within the vertical canopy profile. *Tree Physiology* **21**: 951–958.

Kunert N, Aparecido LMT, Wolff S, Higuchi N, Santos J dos, Araujo AC de, Trumbore S. **2017**. A revised hydrological model for the Central Amazon: The importance of emergent canopy trees in the forest water budget. *Agricultural and Forest Meteorology* **239**: 47–57.

Larjavaara M, Muller-Landau HC. **2013**. Measuring tree height: A quantitative comparison of two common field methods in a moist tropical forest. *Methods in Ecology and Evolution* **4**: 793–801.

Liu H, Gleason SM, Hao G, Hua L, He P, Goldstein G, Ye Q. **2019**. Hydraulic traits are coordinated with maximum plant height at the global scale. *Science Advances* **5**: eaav1332.

Liu Y, Muller RN. **1993**. Effect of Drought and Frost on Radial Growth of Overstory and Undesrstory Stems in a Deciduous Forest. *The American Midland Naturalist* **129**: 19–25.

Lloret F, Keeling EG, Sala A. **2011**. Components of tree resilience: Effects of successive low-growth episodes in old ponderosa pine forests. *Oikos* **120**: 1909–1920.

Lunch C, Laney C, Mietkiewicz N, Sokol E, Cawley K, NEON (National Ecological Observatory Network). **2020**. *NeonUtilities: Utilities for working with neon data.*

Maréchaux I, Bartlett MK, Sack L, Baraloto C, Engel J, Joetzjer E, Chave J. **2015**. Drought tolerance as predicted by leaf water potential at turgor loss point varies strongly across species within an Amazonian forest. *Functional Ecology* **29**: 1268–1277.

Maréchaux I, Saint-André L, Bartlett MK, Sack L, Chave J. **2019**. Leaf drought tolerance cannot be inferred from classic leaf traits in a tropical rainforest (P Mariotte, Ed.). *Journal of Ecology.*

Martin-Benito D, Pederson N. **2015**. Convergence in drought stress, but a divergence of climatic drivers across a latitudinal gradient in a temperate broadleaf forest. *Journal of Biogeography* **42**: 925–937.

Martin-Benito D, Pederson N. **2015**. Convergence in drought stress, but a divergence of climatic drivers across a latitudinal gradient in a temperate broadleaf forest. *Journal of Biogeography* **42**: 925–937.

Mazerolle MJ, Dan Linden. **2019**. *AICcmodavg: Model selection and multimodel inference based on (q)AIC(c).*

McDowell NG, Allen CD. **2015**. Darcy's law predicts widespread forest mortality under climate warming. *Nature Climate Change* **5**: 669–672.

McDowell NG, Allen CD, Anderson-Teixeira K, Aukema BH, Bond-Lamberty B, Chini L, Clark JS, Dietze M, Grossiord C, Hanbury-Brown A ***et al.*** **2020**. Pervasive shifts in forest dynamics in a changing world. *Science* **368**.

McDowell NG, Bond BJ, Dickman LT, Ryan MG, Whitehead D. **2011**. Relationships Between Tree Height and Carbon Isotope Discrimination. In: Meinzer FC, Lachenbruch B, Dawson TE, eds. Tree Physiology. Size- and Age-Related Changes in Tree Structure and Function. Dordrecht: Springer Netherlands, 255–286.

Meakem V, Tepley AJ, Gonzalez-Akre EB, Herrmann V, Muller-Landau HC, Wright SJ, Hubbell SP, Condit R, Anderson-Teixeira KJ. **2018**. Role of tree size in moist tropical forest carbon cycling and water deficit responses. *New Phytologist* **219**: 947–958.

Medeiros CD, Scoffoni C, John GP, Bartlett MK, Inman-Narahari F, Ostertag R, Cordell S, Giardina C, Sack L. **2019**. An extensive suite of functional traits distinguishes Hawaiian wet and dry forests and enables prediction of species vital rates. *Functional Ecology* **33**: 712–734.

Meinzer FC, Andrade JL, Goldstein G, Holbrook NM, Cavelier J, Wright SJ. **1999**. Partitioning of soil water among canopy trees in a seasonally dry tropical forest. *Oecologia* **121**: 293–301.

Mencuccini M. **2003**. The ecological significance of long-distance water transport: Short-term regulation, long-term acclimation and the hydraulic costs of stature across plant life forms. *Plant, Cell & Environment* **26**: 163–182.

Merlin M, Perot T, Perret S, Korboulewsky N, Vallet P. **2015**. Effects of stand composition and tree size on resistance and resilience to drought in sessile oak and Scots pine. *Forest Ecology and Management* **339**: 22–33.

Metcalfe P, Beven K, Freer J. **2018**. *Dynatopmodel: Implementation of the dynamic topmodel hydrological model.*

NEON. **2018**. National Ecological Observatory Network. 2016, 2017, 2018. Data Products: DP1.00001.001, DP1.00098.001, DP1.00002.001. Provisional data downloaded from http://data.neonscience.org/ in May 2019. Battelle, Boulder, CO, USA.

Olson ME, Anfodillo T, Rosell JA, Petit G, Crivellaro A, Isnard S, León-Gómez C, Alvarado-Cárdenas LO, Castorena M. **2014**. Universal hydraulics of the flowering plants: Vessel diameter scales with stem length across angiosperm lineages, habits and climates. *Ecology Letters* **17**: 988–997.

Olson M, Rosell JA, Martínez-Pérez C, León-Gómez C, Fajardo A, Isnard S, Cervantes-Alcayde MA, Echeverría A, Figueroa-Abundiz VA, Segovia-Rivas A ***et al.*** **2020**. Xylem vessel-diameter–shoot-length scaling: Ecological significance of porosity types and other traits. *Ecological Monographs* **n/a**.

Olson ME, Soriano D, Rosell JA, Anfodillo T, Donoghue MJ, Edwards EJ, León-Gómez C, Dawson T, Martínez JJC, Castorena M ***et al.*** **2018**. Plant height and hydraulic vulnerability to drought and cold. *Proceedings of the National Academy of Sciences* **115**: 7551–7556.

Phillips NG, Ryan MG, Bond BJ, McDowell NG, Hinckley TM, Čermák J. **2003**. Reliance on stored water increases with tree size in three species in the Pacific Northwest. *Tree Physiology* **23**: 237–245.

Powell TL, Wheeler JK, Oliveira AAR de, Costa ACL da, Saleska SR, Meir P, Moorcroft PR. **2017**. Differences in xylem and leaf hydraulic traits explain differences in drought tolerance among mature Amazon rainforest trees. *Global Change Biology* **23**: 4280–4293.

Powers JS, G GV, Brodribb TJ, Schwartz NB, Pérez-Aviles D, Smith-Martin CM, Becknell JM, Aureli F, Blanco R, Calderón-Morales E ***et al.*** **2020**. A catastrophic tropical drought kills hydraulically vulnerable tree species. *Global Change Biology* **26**: 3122–3133.

Pretzsch H, Schütze G, Biber P. **2018**. Drought can favour the growth of small in relation to tall trees in mature stands of Norway spruce and European beech. *Forest Ecosystems* **5**: 20.

R Core Team. **2019**. *R: A language and environment for statistical computing*. Vienna, Austria: R Foundation for Statistical Computing.

Rey-Sánchez AC, Slot M, Posada JM, Kitajima K. **2016**. Spatial and seasonal variation in leaf temperature within the canopy of a tropical forest. *Climate Research* **71**: 75–89.

Rosas T, Mencuccini M, Barba J, Cochard H, Saura-Mas S, Martínez-Vilalta J. **2019**. Adjustments and coordination of hydraulic, leaf and stem traits along a water availability gradient. *New Phytologist* **223**: 632–646.

Roskilly B, Keeling E, Hood S, Giuggiola A, Sala A. **2019**. Conflicting functional effects of xylem pit structure relate to the growth-longevity trade-off in a conifer species. *PNAS. doi: /10.1073/pnas.1900734116.*

Ryan MG, Phillips N, Bond BJ. **2006**. The hydraulic limitation hypothesis revisited. *Plant, Cell & Environment* **29**: 367–381.

Sapes G, Roskilly B, Dobrowski S, Maneta M, Anderegg WRL, Martinez-Vilalta J, Sala A. **2019**. Plant water content integrates hydraulics and carbon depletion to predict drought-induced seedling mortality. *Tree Physiology* **39**: 1300–1312.

Scharnweber T, Heinze L, Cruz-García R, Maaten-Theunissen M van der, Wilmking M. **2019**. Confessions of solitary oaks: We grow fast but we fear the drought. *Dendrochronologia* **55**: 43–49.

Scholz FG, Phillips NG, Bucci SJ, Meinzer FC, Goldstein G. **2011**. Hydraulic Capacitance: Biophysics and Functional Significance of Internal Water Sources in Relation to Tree Size. In: Meinzer FC, Lachenbruch B, Dawson TE, eds. Tree Physiology. Size- and Age-Related Changes in Tree Structure and Function. Dordrecht: Springer Netherlands, 341–361.

Schöngart J, Bräuning A, Barbosa ACMC, Lisi CS, Oliveira JM de. **2017**. Dendroecological Studies in the Neotropics: History, Status and Future Challenges. In: Amoroso MM, Daniels LD, Baker PJ, Camarero JJ, eds. Ecological Studies. Dendroecology: Tree-Ring Analyses Applied to Ecological Studies. Cham: Springer International Publishing, 35–73.

Scoffoni C, Vuong C, Diep S, Cochard H, Sack L. **2014**. Leaf Shrinkage with Dehydration: Coordination with Hydraulic Vulnerability and Drought Tolerance. *Plant Physiology* **164**: 1772–1788.

Simeone C, Maneta MP, Holden ZA, Sapes G, Sala A, Dobrowski SZ. **2019**. Coupled ecohydrology and plant hydraulics modeling predicts ponderosa pine seedling mortality and lower treeline in the US Northern Rocky Mountains. *New Phytologist* **221**: 1814–1830.

Slette IJ, Post AK, Awad M, Even T, Punzalan A, Williams S, Smith MD, Knapp AK. **2019**. How ecologists define drought, and why we should do better. *Global Change Biology* **0**: 1–8.

Stahl C, Hérault B, Rossi V, Burban B, Bréchet C, Bonal D. **2013**. Depth of soil water uptake by tropical rainforest trees during dry periods: Does tree dimension matter? *Oecologia* **173**: 1191–1201.

Stovall AEL, Anderson-Teixeira KJ, Shugart HH. **2018a**. Terrestrial LiDAR-derived non-destructive woody biomass estimates for 10 hardwood species in Virginia. *Data in Brief* **19**: 1560–1569.

Stovall AEL, Anderson-Teixeira KJ, Shugart HH. **2018b**. Assessing terrestrial laser scanning for developing non-destructive biomass allometry. *Forest Ecology and Management* **427**: 217–229.

Stovall AEL, Shugart H, Yang X. **2019**. Tree height explains mortality risk during an intense drought. *Nature Communications* **10**: 1–6.

Stovall AEL, Shugart HH, Yang X. **2020**. Reply to 'Height-related changes in forest composition explain increasing tree mortality with height during an extreme drought'. *Nature Communications* **11**: 3401.

Suarez ML, Ghermandi L, Kitzberger T. **2004**. Factors predisposing episodic drought-induced tree mortality in Nothofagus– site, climatic sensitivity and growth trends. *Journal of Ecology* **92**: 954–966.

Sørensen R, Zinko U, Seibert J. **2006**. On the calculation of the topographic wetness index: Evaluation of different methods based on field observations. *Hydrology and Earth System Sciences* **10**: 101–112.

Trenberth KE, Dai A, Schrier G van der, Jones PD, Barichivich J, Briffa KR, Sheffield J. **2014**. Global warming and changes in drought. *Nature Climate Change* **4**: 17–22.

Trugman AT, Detto M, Bartlett MK, Medvigy D, Anderegg WRL, Schwalm C, Schaffer B, Pacala SW. **2018**. Tree carbon allocation explains forest drought-kill and recovery patterns. *Ecology Letters* **21**: 1552–1560.

Vitasse Y, Bottero A, Cailleret M, Bigler C, Fonti P, Gessler A, Lévesque M, Rohner B, Weber P, Rigling A ***et al.*** **2019**. Contrasting resistance and resilience to extreme drought and late spring frost in five major European tree species. *Global Change Biology* **25**: 3781–3792.

Wheeler EA, Baas P, Rodgers S. **2007**. Variations In Dieot Wood Anatomy: A Global Analysis Based on the Insidewood Database. *IAWA Journal* **28**: 229–258.

Zach A, Schuldt B, Brix S, Horna V, Culmsee H, Leuschner C. **2010**. Vessel diameter and xylem hydraulic conductivity increase with tree height in tropical rainforest trees in Sulawesi, Indonesia. *Flora - Morphology, Distribution, Functional Ecology of Plants* **205**: 506–512.

Zellweger F, Coomes D, Lenoir J, Depauw L, Maes SL, Wulf M, Kirby KJ, Brunet J, Kopecký M, Máliš F ***et al.*** **2019**. Seasonal drivers of understorey temperature buffering in temperate deciduous forests across Europe. *Global Ecology and Biogeography* **28**: 1774–1786.

Zhu S-D, Chen Y-J, Ye Q, He P-C, Liu H, Li R-H, Fu P-L, Jiang G-F, Cao K-F. **2018**. Leaf turgor loss point is correlated with drought tolerance and leaf carbon economics traits. *Tree Physiology* **38**: 658–663.

Zuleta D, Duque A, Cardenas D, Muller-Landau HC, Davies SJ. **2017**. Drought-induced mortality patterns and rapid biomass recovery in a terra firme forest in the Colombian Amazon. *Ecology* **98**: 2538–2546.

Table 1. Summary of hypotheses, corresponding specific predictions, and results.

Hypotheses & Specific Predictions	Prediction supported?				Results
		tree-ring drought records			
	recent non-drought conditions	Resistance (Rt)	Recovery (Rc)	Resilience (Rs)	
Tree size and microenvironment					
Across the forest vertical profile, taller trees are exposed to higher evaporative demand.					
Taller trees experience higher wind speeds during the peak growing season months.	yes				Fig. 2
Taller trees experience lower humidity during the peak growing season months.	yes				Fig. 2
Taller trees experience higher air temperatures during the peak growing season months.	no				Fig. 2
Taller trees have more sun-exposed crowns.	yes				Fig. 2
At least within the forest setting, taller trees are less drought tolerant.					
Drought tolerance decreases with height (H).		yes	yes	yes	Fig. 4; Tables S8-S11
Small trees (lower root volume) in drier microhabitats have lower drought tolerance.					
There is a negative interactive effect between H and topographic wetness index.		(no)	(yes)	(yes)	Tables S8-S11
Species traits					
Species' traits–particularly leaf drought tolerance traits–predict drought tolerance.					
Wood density correlates (positively or negatively) to drought tolerance.		-	-	-	Tables S4-S7
Leaf mass per area correlates positively to drought tolerance.		-	-	-	Tables S4-S7
Ring-porous species have higher drought tolerance than diffuse- or semi-ring- porous.		-	no	-	Tables S4-S7
Percent loss leaf area upon desiccation correlates negatively with drought tolerance.		yes	(yes)	(yes)	Fig. 4; Tables S8-S11
Water potential at turgor loss correlates negatively with drought tolerance.		(yes)	(yes)	(yes)	Fig. 4; Tables S8-S11

Parentheses indicate that the prediction was supported by at least one but not all of the top models (Tables S8, S10, S11). Dash symbols indicate that the response was not significant (Tables S4, S6, S7).

Table 2. Overview of analyzed species, listed in order of their relative contributions to woody stem productivity ($ANPP_{stem}$) in the plot, along with numbers and sizes sampled, and species traits.

			contemporary DBH (cm)		species traits (mean +/- se)				
species	% $ANPP_{stem}$	n trees*	mean	range	WD ($g\,cm^{-3}$)	LMA ($g\,cm^{-2}$)	xylem porosity	π_{tlp} (Mpa)	PLA_{dry} (%)
Liriodendron tulipifera L. (LITU)	47.1	98	36.9	10 - 100.4	0.4 ± 0.03	46.9 ± 12.4	diffuse	-1.92 ± 0.17	19.6 ± 2.06
Quercus alba L. (QUAL)	10.7	61	47.2	11.4 - 79.1	0.61 ± 0.02	75.8 ± 11.1	ring	-2.58 ± 0.08	8.52 ± 0.37
Quercus rubra L. (QURU)	10.1	69	54.9	11.1 - 148	0.62 ± 0.02	71.1 ± 6.70	ring	-2.64 ± 0.28	11.0 ± 0.84
Quercus velutina Lam. (QUVE)	7.8	77	54.1	16.0 - 114.2	0.65 ± 0.04	48.7 ± 3.30	ring	-2.39 ± 0.15	13.42 ± 0.84
Quercus montana L. (QUPR)	4.8	59	42.3	10.5 - 87.2	0.61 ± 0.01	71.8 ± 40.2	ring	-2.36 ± 0.09	11.75 ± 1.37
Fraxinus americana L. (FRAM)	3.8	62	35.4	6.4 - 94.7	0.56 ± 0.01	43.3 ± 4.78	ring	-2.1 ± 0.36	13.06 ± 1.06
Carya glabra (Mill.) Sweet (CAGL)	3.7	31	31.4	9.8 - 98.5	0.62 ± 0.04	42.8 ± 0.94	ring	-2.13 ± 0.50	21.09 ± 5.48
Juglans nigra L. (JUNI)	2.1	31	48.1	24.2 - 87	1.09 ± 0.09	72.1 ± 7.10†	semi-ring	-2.76 ± 0.21	24.64 ± 8.72
Carya cordiformis (Wangenh.) K. Koch (CACO)	2.0	13	27.2	10.7 - 61.5	0.83 ± 0.10	45.9 ± 15.6	ring	-2.13 ± 0.45	17.22 ± 2.25
Carya tomentosa (Lam. ex Poir.) Nutt. (CATO)	2.0	13	21.0	12.1 - 32.2	0.83	45.4	ring	-2.2	16.56
Fagus grandifolia Ehrh. (FAGR)	1.5	80	23.5	11.2 - 107.2	0.62 ± 0.03	30.7 ± 4.94	diffuse	-2.57	9.45 ± 1.25
Carya ovalis (Wangenh.) Sarg. (CAOVL)	1.1	23	35.3	14.9 - 66.0	0.96 ± 0.33	47.6 ± 3.95	ring	-2.48 ± 0.04	14.8 ± 6.34

* Numbers cored live versus dead are given in Table S1 of Helcoski et al. (2019).

† Semi-ring porosity is intermediate between ring and diffuse. We group it with diffuse-porous species for more even division of species between categories.

Variable abbreviations are as in Table 3. DBH measurements are from the most recent ForestGEO census in 2018 (live trees) or tree mortality censuses in 2016 and 2017 (trees cored dead).

Table 3. Summary of dependent and independent variables in our statistical models of drought tolerance, along with units, definitions, and sample sizes.

variable	symbol	units	description	category	n_{Rt}*	n_{Rc}	n_{Rs}
Dependent variables							
drought resistance	Rt	-	ratio of basal area increment (BAI) during drought year to mean BAI of the 5 years prior.	-	1623	-	-
	Rt_{ARIMA}	-	ratio of BAI during drought year to BAI predicted by ARIMA model.	-	1654	-	-
drought recovery	Rc	-	ratio of mean BAI for 5 years after drought to BAI during drought year.	-	-	1557	-
drought resilience	Rs	-	ratio of mean BAI for 5 years after drought to mean BAI for 5 years before drought.	-	-	-	1570
Independent variables							
drought year	Y	-	year of drought	1966	513	491	495
				1977	543	524	523
				1999	567	542	552
height	H	m	estimated H in drought year	-	-	-	-
topographic wetness index	TWI	-	steady-state wetness index based on slope and upstream contributing area	-	-	-	-
species' traits							
wood density	WD	g cm^{-3}	dry mass of a unit volume of fresh wood	-	-	-	-
leaf mass per area	LMA	kg m^{-2}	ratio of leaf dry mass to fresh leaf area	-	-	-	-
xylem porosity		-	vessel arrangement in xylem	ring (R)	1106	1079	1088
				semi-ring (SR)	81	73	78
				diffuse (D)	436	405	404
turgor loss point	π_{tlp}	MPa	water potential at which leaves wilt	-	-	-	-
percent loss area	PLA_{dry}	%	percent loss of leaf area upon dessication	-	-	-	-

Sample sizes are after removal of outliers. Dashes for sample sizes of independent variables indicate that the variable was available for all records. Xylem porosity sample sizes are sums across all drought years.

*Sample sizes of independent variables refer to the Rt model.

Figure Legends

Figure 1. Climate and species-level growth responses over our study period, highlighting the three focal drougths (a) and community-wide growth resistance, Rt (b), and resilience, Rs (c). Time series plot (a) shows peak growing season (May-August) climate conditions and residual chronologies for each species (see Table 3 for codes). PET and PRE data were obtained from the Climatic Research Unit high-resolution gridded dataset (CRU TS v.4.01; Harris et al. 2014). Focal droughts are indicated by dashed lines, and shading indicates the pre- and post- drought periods used in calculations of the resistance metric. Figure modified from Helcoski *et al.* (2019). Density plots (b-c) show the distribution of Rt and Rs values for each drought. See Fig. S6 for parallel plot for recovery (Rc).

Figure 2. Contemporary height profiles in sun exposure and growing season microclimate under non-drought conditions. Shown are average (± SD) of daily maxima and minima of (a) wind speed, (b) relative humidity (RH), and (c) air temperature (T_{air}) averaged over each month of the peak growing season (May-August) from 2016-2018. In these plots, heights are slightly offset for visualization purposes. Asterisks indicate significant differences between the top and bottom of the height profile. Also shown is (d) tree heights by 2018 crown position, with letters indicating significance groupings. In all plots, the dashed horizontal line indicates the 95th percentile of tree heigts in the ForestGEO plot.

Figure 3. Drought resistance, Rt (a), and resilience, Rs (b), across species for the three focal droughts. Species codes are given in Table 2. See Fig. S7 for parallel plot for recovery (Rc). Analysis conducted using *agricolae* package (de Mendiburu, 2020).

Figure 4. Visualization of best statistical models for drought resistance (Rt), recovery (Rc), and resilience (Rs) for all droughts combined and for each individual drought year. Confidence intervals were defined via bootsrapping in the bootpredictlme4 package. Model coefficients are given in Tables S8 and S10-11.

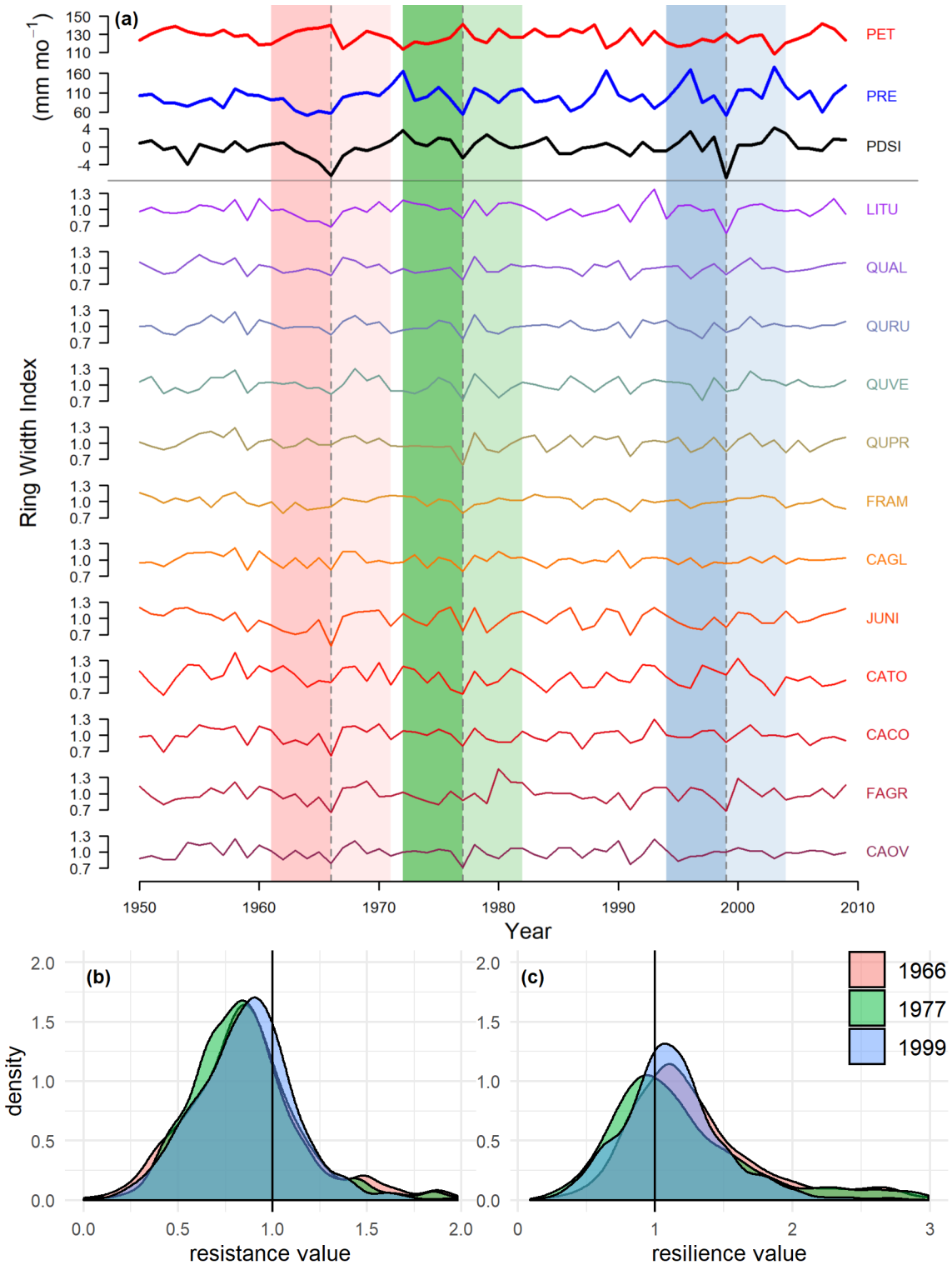

Figure 1. Climate and species-level growth responses over our study period, highlighting the three focal drougths (a) and community-wide growth resistance, *Rt* (b), and resilience, *Rs* (c). Time series plot (a) shows peak growing season (May-August) climate conditions and residual chronologies for each species (see Table 3 for codes). PET and PRE data were obtained from the Climatic Research Unit high-resolution gridded dataset (CRU TS v.4.01; Harris et al. 2014). Focal droughts are indicated by dashed lines, and shading indicates the pre- and post- drought periods used in calculations of the resistance metric. Figure modified from Helcoski *et al.* (2019). Density plots (b-c) show the distribution of *Rt* and *Rs* values for each drought. See Fig. S6 for parallel plot for recovery (*Rc*).

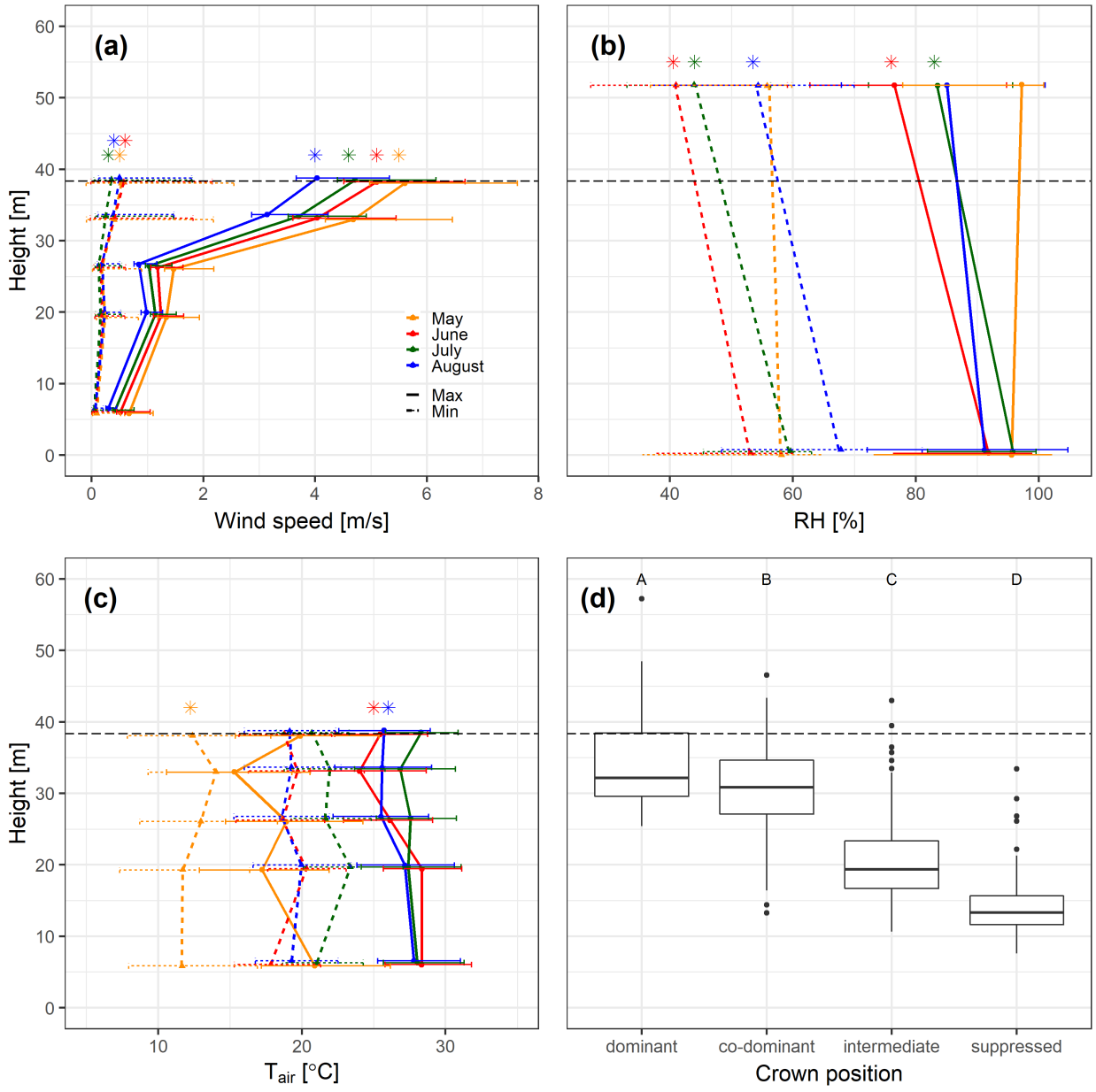

Figure 2. Contemporary height profiles in sun exposure and growing season microclimate under non-drought conditions. Shown are average (± SD) of daily maxima and minima of (a) wind speed, (b) relative humidity (RH), and (c) air temperature (T_{air}) averaged over each month of the peak growing season (May-August) from 2016-2018. In these plots, heights are slightly offset for visualization purposes. Asterisks indicate significant differences between the top and bottom of the height profile. Also shown is (d) tree heights by 2018 crown position, with letters indicating significance groupings. In all plots, the dashed horizontal line indicates the 95th percentile of tree heigts in the ForestGEO plot.

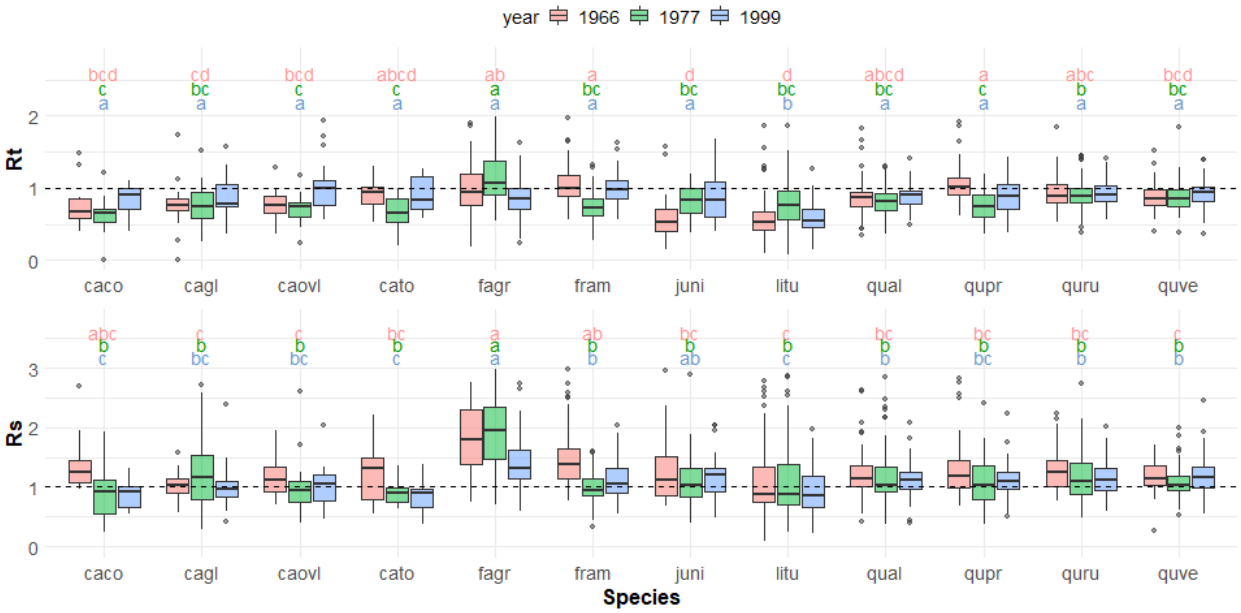

Figure 3. Drought resistance, *Rt* (a), and resilience, *Rs* (b), across species for the three focal droughts. Species codes are given in Table 2. See Fig. S7 for parallel plot for recovery (*Rc*).

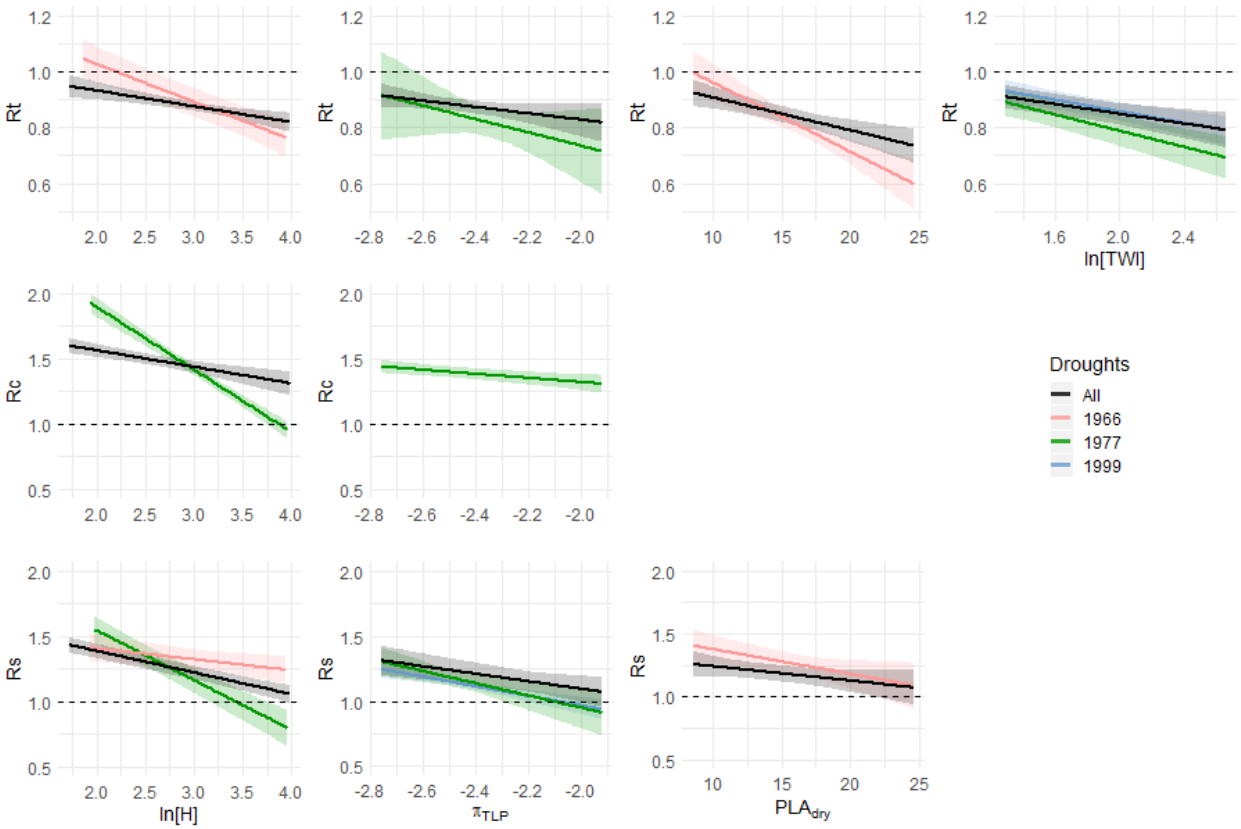

Figure 4. Visualization of top statistical models for drought resistance (*Rt*), recovery (*Rc*), and resilience (*Rs*) for all droughts combined and for each individual drought year. For cases where the best model includes a DBH x TWI interaction (*Rc* in all droughts and 1966, *Rs* in all droughts and 1977), we plot the best model without the interaction. Visualization of the best mixed effects model per drought scenario was created by the visreg package (Breheny and Burchett, 2020), and confidence intervals were defined via bootsrapping in the bootpredictlme4 package. Model coefficients are given in Tables S8 and S10-11.